Ab Initio Determination of Dark Structures in Radiationless Transitions for Aromatic Carbonyl Compounds

WEI-HAI FANG*

College of Chemistry, Beijing Normal University, Beijing 100875, China

RECEIVED ON SEPTEMBER 15, 2007

CONSPECTUS

Mechanistic photodissociation of a polyatomic molecule has long been regarded as an intellectually challenging area of chemical physics, the results of which are relevant to atmospheric chemistry, biological systems, and many application fields. Carbonyl compounds play a unique role in the development of our understanding of the spectroscopy, photochemistry, and photophysics of polyatomic molecules and their photodissociation has been the subject of numerous studies over many decades. Upon irradiation, a molecule can undergo internal conversion (IC) and intersystem crossing (ISC) processes, besides photochemical and other photophysical processes. Transient intermediates formed in the IC and ISC radiationless processes, which are termed "dark", are not amenable to detection by conventional light absorption or emission. However, these dark intermediates play critical roles in IC and ISC processes and thus are essential to understanding mechanistic photochemistry of a polyatomic molecule. We have applied the multiconfiguration complete active space self-consistent field (CASSCF) method to determine the dark transient structures involved in radiationless processes for acetophenone and the related aromatic carbonyl compounds. The electronic and geometric structures predicted for the dark states are in a good agreement with those determined by ultrafast electron diffraction experiments. Intersection structure of different electronic states provides a very efficient "funnel" for the IC or ISC process. However, experimental determination of the intersection structure involved in radiationless transitions of a polyatomic molecule is impossible at present. We have discovered a minimum energy crossing point among the three potential energy surfaces (S_1, T_1, and T_2) that appears to be common to a wide variety of aromatic carbonyl compounds with a constant structure. This new type of crossing point holds the key to understanding much about radiationless processes after photoexcitation of aromatic carbonyl compounds. The importance of ab initio determination of transient structures in the photodissociation dynamics has been demonstrated for the case of the aromatic carbonyl compounds. In addition, the detailed knowledge of mechanistic photochemistry for aromatic carbonyl compounds forms the basis for further investigating photodissociation dynamics of a polyatomic molecule.
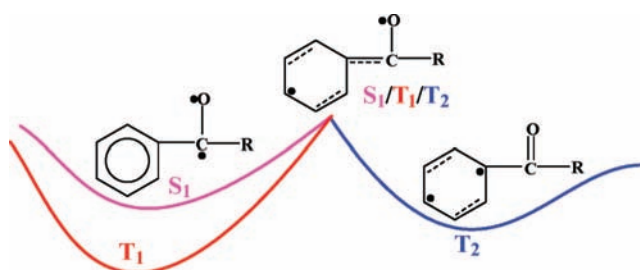
Introduction

Mechanistic photochemistry of a polyatomic molecule has long been regarded as an intellectually challenging area of chemical physics,[1] the results of which are relevant to atmospheric chemistry,[2–4] biological systems,[5–7] and some other processes.[8–10] Photodissociation of carbonyl compounds has served as the basis for developing new experimental methods for direct observation of transient intermediates[11–13] and for discovering new mechanisms of photochemical reactions.[14,15] Photoexcitation ($n \rightarrow \pi^*$) of a ketone from the ground state (S_0) to its first excited singlet state (S_1) may lead to breakage of a bond α to the carbonyl group, which is known as Norrish type I reaction. When a ketone contains γ-C—H bonds, the 1,5-hydrogen shift reaction can also take place, yielding a

1,4-biradical. This biradical can either react by cleavage or by cyclization or undergo back-hydrogen transfer to yield the starting material. These processes are referred to as Norrish type II reaction.[16] It was suggested in early experimental studies that the weaker of the two α-C—C bonds is cleaved preferentially upon n $\rightarrow$ π^* excitation of asymmetrically substituted aliphatic ketones. However, the stronger α bond was observed to break preferentially in recent experiments.[17,18] A series of theoretical studies[19−21] indicated that the bond strength is only one factor that influences the selectivity of the α bond fissions and the selectivity is mainly dependent on the cleavage mechanism. The conjugation interaction between the aromatic ring and the carbonyl group has a noticeable influence on the relative energies of the nπ^* and $\pi\pi^*$ states as well as their chemical reactivity. Therefore, the relaxation dynamics and dissociation mechanisms for the excited aromatic carbonyl molecules are different from those for aliphatic carbonyl compounds. Experimentally, it has been well established that both singlet and triplet nπ^* states can undergo Norrish type I and II reactions for aliphatic ketones.[22−28] However, both reactions occur only from the lowest triplet state for most aromatic ketones or aldehydes. The excited singlet state lifetime for aromatic ketones has been found to be much shorter than that for the corresponding aliphatic ketones in both the gas and condensed phases.[22−28] Aromatic carbonyl compounds are highly phosphorescent but only weakly fluorescent molecules.

After light absorption, a molecule can undergo radiationless processes of two general types: photochemical, involving bond fragmentation or isomerization, and photophysical, involving transitions between electronic states while either conserving spin (internal conversion) or altering spin (intersystem crossing). Internal conversion (IC) and intersystem crossing (ISC) play an important role in mechanism and dynamics of photochemical reactions. For more than eight decades, our understanding of such radiationless processes has come from indirect evidence based on yields and decay rates of the radiative population. With the advent of picosecond and femtosecond time resolution, it became possible to study the time scale of radiationless processes and to resolve the actual nuclear motions in these processes.[11] However, the intermediate structures formed through radiationless transitions, which are termed "dark", are not amenable to detection by conventional light absorption or emission. Optically dark structures can be observed by means of ultrafast electron diffraction developed recently by Zewail and co-workers,[12,13] but the unique techniques and the related complex theory make the dark transient structures determined by ultrafast electron dif-

fraction a challenge to experimental chemists. Great strides have been made in the ability to carry out accurate quantum mechanical calculations for static molecular structures, due to enhanced computational power and significant methodological advances. The multiconfiguration complete active space self-consistent field (CASSCF), multiconfiguration second-order perturbation theory (CASPT2), and multireference configuration interaction (MR-CI) methods are increasingly becoming a powerful tools in study of excited-state structure and properties. We have applied the CASSCF method to determine the dark transient structures involved in radiationless processes of acetophenone and the related aromatic carbonyl compounds.[29−32] The electronic and geometric structures predicted for the dark states are in a good agreement with those determined by ultrafast electron diffraction experiments.[11−13] Intersection structures of different electronic states that provide a very efficient "funnel" for the IC and ISC processes can be determined with high-level ab initio calculations. However, experimental determination of the intersection structure involved in radiationless transitions of a polyatomic molecule is impossible at present. We have discovered a minimum energy crossing point among the three potential energy surfaces (S_1, T_1, and T_2) that appears to be common to a wide variety of aromatic carbonyl compounds with a constant structure. This new type of crossing point holds the key to understanding much about radiationless processes after photoexcitation of aromatic carbonyl compounds.

Computational Strategy

The multireference configuration interaction (MR-CI) and multiconfiguration second-order perturbation theory (CASPT2) are very efficient algorithms in treating electronic correlation. But it is a difficult task, at present, to optimize a stationary structure at the MR-CI and CASPT2 levels of theory for a moderate-size molecule, such as acetophenone. The CASSCF wave function has sufficient flexibility to model the changes in electronic structure upon electronic excitations. The CASSCF method can provide a balanced description of the stationary structures on the ground and excited states, but the selection of the active space is a crucial step. For acetophenone, the active space should be composed of three π and three π^* orbitals in the aromatic ring, the C—O π and π^* orbitals, and the oxygen nonbonding orbital. In this case, the near-degenerate orbitals are included in the active space, which can provide a good description on structures and the relative energies. This will be discussed below.

In principle, the third root of the CI matrix should be sought in order to describe the second excited singlet state (S_2) of a

SCHEME 1
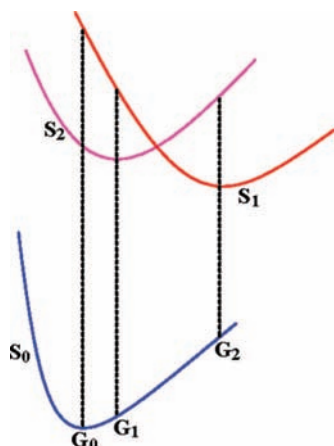
system without any symmetry. However, the error in the calculated relative energies is sharply increased with the number of roots. In addition, the CASSCF convergence becomes very difficult for high excited states. As a result, a correct prediction of high excited states (S_2, T_2, ...) requires a distinctive technique of computation. As shown in Scheme 1, energy order of an excited electronic state varies with geometric structures. The S_2 minimum is definitely higher than the S_1 minimum in energy, but the S_2 state is energetically lower than the S_1 state at some nuclear configurations, such as G_0 and G_1 in Scheme 1. If the initial structure is chosen to be near G_1, the S_2 state becomes the lowest excited singlet state and can be solved as the second root of the CI matrix. For acetophenone and the related aromatic carbonyl compounds, the singlet and triplet $\pi\pi^*$ states are mainly localized at the aromatic ring, while the singlet and triplet $n\pi^*$ states correspond to a local excitation at the carbonyl group. A large difference exists in electronic and geometric structures of the $n\pi^*$ and $\pi\pi^*$ states for aromatic carbonyl compounds. As a result, the $\pi\pi^*$ singlet state ($^1\pi\pi^*$) is lower than the $n\pi^*$ singlet state at the $^1\pi\pi^*$ equilibrium geometry. Therefore, the S_2 state ($^1\pi\pi^*$) can be treated as the lowest excited singlet state, on the condition that initial molecular orbitals and starting geometry are chosen correctly. In this way, structural optimization and energy calculation for the $^1\pi\pi^*$ state can be performed with high accuracy.

Equilibrium Geometries

As pointed out before, the dark structures involved in radiationless processes are difficult to detect experimentally. But these structures can be accurately predicted by means of the advanced ab initio techniques. On the basis of the CASSCF molecular orbitals and their populations, the S_1, T_1, S_2, and T_2 excited states were, respectively, assigned as $^1n\pi^*$, $^3n\pi^*$, $^1\pi\pi^*$

TABLE 1. The Selected Bond Lengths (Å) for the Dark T_2 and $S_1/T_2/T_1$ Structures of Benzaldehyde (BA) and Acetophenone (PA)

| | T_2 | | | | $S_1/T_2/T_1$ | |
| | BA | | PA | | BA | PA |
	calc[a]	expt[b]	calc[a]	expt[b]	calc[a]	calc[a]
C_1-C_2[c]	1.483	1.479 ± 0.029	1.486	1.495 ± 0.014	1.469	1.470
C_2-C_3	1.362	1.322 ± 0.029	1.361	1.349 ± 0.021	1.335	1.335
C_3-C_4	1.442	1.487	1.445	1.441	1.449	1.449
C_4-C_5	1.459	1.487	1.460	1.441	1.422	1.421
C_5-C_6	1.358	1.322 ± 0.029	1.358	1.349 ± 0.021	1.370	1.371
C_6-C_1	1.471	1.479 ± 0.029	1.474	1.495 ± 0.014	1.469	1.470
C_1-C_7	1.419	1.420 ± 0.045	1.441	1.460	1.382	1.393
C_7-O_8	1.239	1.263 ± 0.031	1.233	1.214 ± 0.018	1.305	1.304

[a] The CASSCF calculated values from refs 29 and 31. [b] The experimental values from refs 12 and 13. [c] The atom numbering is given in Scheme 2.

SCHEME 2
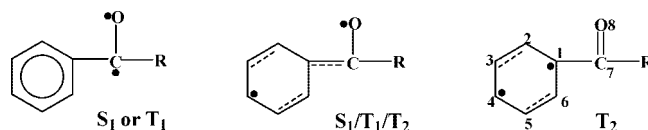
and $^3\pi\pi^*$ in nature for acetophenone and the related aromatic carbonyl compounds (C_6H_5COR, R = H, CH_3, CH_2CH_3, and $CH_2CH_2CH_3$).[29–32] The CASSCF-optimized bond parameters for these carbonyl molecules in the five lowest electronic states have been reported in the previous calculations.[29–32] For comparison, the C—C and C—O bond lengths for benzaldehyde and acetophenone in the T_2 state are listed in Table 1, where the available experimental values are also given. In the ground state, the aromatic ring was predicted to be almost a regular hexagon with the C—C—C angle in the range of 119.8°–120.3° and the largest difference of 0.012 Å in the ring C—C bond length. With respect to the S_0 structure, the most striking change in the T_1 or S_1 structure is associated with the C—O bond length. The C—O bond length is ~1.21 Å in the ground state, and it becomes ~1.35 Å in the T_1 or S_1 structure. The n → π^* transition of the C_6H_5COR molecule is dominated by progression in the C=O stretching mode, which reflects substantial change in the C—O bond length and has a little influence on the structure of the aromatic ring. The S_1 and T_1 electronic states are of similar biradical character, which is described in Scheme 2. As expected, the π → π^* transition is mainly localized in the aromatic ring, and this transition has a large influence on structures of the aromatic ring, but the carbonyl group is less influenced by the π → π^* transition. Two unpaired electrons of the S_2 state are delocalized into the whole aromatic ring, which results in a uniform increase of the ring C—C bonds from ~1.40 Å in S_0 to ~1.44 Å in S_2.

The T_2 state is of biradical character (Scheme 2), but its electronic and geometric structures are quite different from

TABLE 2. The Adiabatic Excitation Energies (eV) for C_6H_5CHO (BA), $C_6H_5COCH_3$ (PA), and $C_6H_5COCH_2CH_3$ (PE)

	BA					PA				PE
	expt[a]	CASSCF[b]	MCSCF[c]	CASPT2[d]	MCQDPT[e]	expt[a]	CASSCF[b]	MCSCF[c]	MCQDPT[e]	CASSCF[b]
S_0	0.0	0.0	0.0	0.0	0.0	0.0	0.0	0.0	0.0	0.0
T_1	3.12	3.13	3.07	3.07	3.09	3.20	3.20	3.17	3.18	3.27
S_1	3.34	3.29	3.29	3.27	3.39	3.38	3.35	3.31	3.38	3.42
T_2	3.30	3.22	3.08	3.16	3.12		3.27	3.11	3.18	3.28
S_2	4.36	4.58	4.46	4.00	4.09	4.39	4.59	4.47	4.13	4.59

[a] Experimentally inferred values from refs 26 and 34. [b] The CASSCF/6-31G* calculated values from ref 31. [c] The MCSCF/6-311G** calculated values from ref 13. [d] The CASPT2 calculated adiabatic excitation energies from ref 35. [e] The MCQDPT calculated adiabatic excitation energies from ref 13.

those for the S_2 state. In the T_2 structure two C—C bonds in the aromatic ring are mainly of double bond character, and the other C—C bond distances are close to the C—C single bond length. Structural dynamics of the aromatic carbonyls benzaldehyde and acetophenone have been studied using the methodology of ultrafast electron diffraction.[11−13] It was found that intersystem crossing in both molecules results in a "quinoidlike" structure for the T_2 state with the excitation being localized in the phenyl ring. The nature of the T_2 electronic structure predicted by the CASSCF calculations is confirmed by the ultrafast electron diffraction experiment. Using the DFT-optimized bond parameters involving hydrogen atoms, Zewail and co-workers fitted the T_2 structure for acetophenone and benzaldehyde from the two-dimensional diffraction data with C_{2v} symmetry imposed for the phenyl ring.[12,13] The C—C and C—O bond lengths inferred experimentally for the T_2 state are given in Table 1. A comparison reveals that the bond parameters optimized by the CASSCF method are well-consistent with those inferred by the ultrafast electron diffraction experiment.

Adiabatic Excitation Energies

As the simplest aromatic aldehyde and ketone, benzaldehyde (C_6H_5CHO) and acetophenone ($C_6H_5COCH_3$) have become the classic aromatic carbonyl molecules for photochemical and spectroscopic studies. The band origins for electronic excitation from S_0 to T_1, S_1, and S_2, which are listed in Table 2, were inferred experimentally. The adiabatic excitation energies were calculated at the CAS(10,9)/6-31G* level[31] as energy difference between the S_0 minimum and the S_1, T_1, S_2, or T_2 minimum, and the obtained results are listed in Table 2, where the CASPT2 and MCQDPT calculated values are given for comparison. In order to explore the influence of alkyl chain length and substituents on the adiabatic transition energy, structures and energies of the S_0, T_1, S_1, T_2, and S_2 states for phenyl ethyl ketone ($C_6H_5COCH_2CH_3$) and *ortho-*, *meta-*, and *para-*CH_3 and *ortho-*, *meta-*, and *para-*Cl substituted $C_6H_5COCH_3$ have been investigated at the CAS(10,9) level with the 6-31G* basis set. Different substituents and sub-

stitution at different positions were found to have little influence on the transition energy, and the adiabatic transition energy to each low-lying electronic state is predicted to be nearly a constant for the investigated aromatic carbonyl compounds.[31,32]

As listed in Table 2, the adiabatic excitation energies to the T_1 and S_1 states for C_6H_5CHO were predicted to be respectively 3.13 and 3.29 eV by the CAS(10,9)/6-31G* calculations, which are very close to the experimentally inferred values of 3.12 and 3.34 eV. Experimentally, great efforts have been devoted to determine the location of the lowest $\pi\pi^*$ triplet state for C_6H_5CHO and $C_6H_5COCH_3$.[26] It is believed that the two triplet states lie close to each other in the region ~2000 cm^{-1} below the S_1 minimum. The T_2 band origin was estimated to be 3.30 eV for C_6H_5CHO. Measurements of the sensitized phosphorescence spectra of jet-cooled acetophenone indicated that the T_2 state is not far from the T_1 state, but the position of T_2 was not definitely determined in the experiment. In comparison with the experimental estimation, the CAS(10,9)/6-31G* calculations provide a good description on the T_2 relative energy of C_6H_5CHO and $C_6H_5COCH_3$. As shown in Table 2, the S_2 origin was overestimated by ~0.2 eV with the CAS(10,9)/6-31G* calculation, and the error is decreased to ~0.1 eV by the MCSCF calculation with the 6-311G** basis set.[13] Although more electron correction is included in the CASPT2 and MCQDPT calculations, the resulting adiabatic excitation energies are not better than those predicted by the CAS(10,9) calculations, as compared with the experimental findings. Analogous results have been obtained in a previous study.[33] The CASSCF calculations with six π electrons in six π orbitals predicted the $S_0 \rightarrow S_1$ transition energy to be 4.61 eV for toluene ($C_6H_5CH_3$), which is very close to the experimentally observed $S_0 \rightarrow S_1$ band origin of 4.65 eV.

The above comparison clearly reveals that the CASSCF calculations provide a very good estimation of the excited-state structures and the adiabatic transition energies for aromatic carbonyl compounds. As pointed out before, for aromatic carbonyl compounds that have relatively large π conjugation systems, π and σ orbitals are well separated in energy. The

CASSCF calculations with near-degenerate π and oxygen non-bonding orbitals included in the active space can accurately predict the excited-state structures and relative energies of aromatic carbonyl compounds. Structures of a series of small organic molecules in the ground and excited states were optimized with the CASSCF and CASPT2 methods.[36] The CASSCF optimized bond parameters are not significantly improved by the CASPT2 calculations, as compared with structures inferred experimentally. However, the CASPT2 geometry optimization is very time-consuming and cannot be completed for a large molecule at present. Actually, the CASSCF method is a good algorithm for treating stationary points on excited-state potential energy surfaces if the active space is chosen correctly.

The $S_1/T_2/T_1$ Three-Surface Intersection

In order to investigate the S_1 relaxation dynamics, we searched for the minimum energy crossing point between the singlet and triplet state surfaces and the crossing point between the two triplet surfaces. It was found that the S_1/T_2 and T_2/T_1 intersections are indistinguishable from one another in structure and the two intersections have the same energy. In fact, the S_1, T_1, and T_2 surfaces intersect in the same region ($S_1/T_2/T_1$) for the aromatic carbonyl compounds.[29–32] The structure of the PhCO moiety is very similar in the $S_1/T_2/T_1$ intersections for all of the aromatic carbonyl compounds investigated so far. The $S_1/T_2/T_1$ surface intersection is likely a common feature for a wide variety of aromatic carbonyl compounds with a nearly constant structure.

As shown in Scheme 2, the $S_1/T_2/T_1$ structure is located between $S_1(T_1)$ and T_2 with the two unpaired electrons distributed in the O atom and the aromatic ring, respectively. The differences between the S_1 and $S_1/T_2/T_1$ structures mainly result from the redistribution of the conjugation of π electrons and thus would not be expected to give rise to a substantial change in energy. The $S_1/T_2/T_1$ structure was predicted to be $4-6$ kcal·mol^{-1} above the S_1 minimum. After photoexcitation to the S_1 state, the relaxation from the S_1 Franck–Condon (FC) geometry to the $S_1/T_2/T_1$ region only involves deformation of the conjugation of the PhCO moiety, and this takes place easily. In view of the structures and the energies found for the FC point on S_1, the S_1 minimum, and the $S_1/T_2/T_1$ intersection, the initially excited wave packet starts from the FC geometry on the S_1 surface and can readily travel to reach the $S_1/T_2/T_1$ intersection.

Direct $S_1(^1n\pi^*) \rightarrow T_1(^3n\pi^*)$ intersystem crossing for carbonyl compounds occurs with a low efficiency because there is no first-order spin–orbit coupling for the $S_1 \rightarrow T_1$ transition.[37] The $S_1 \rightarrow T_1$ ISC rate constant was measured to be $\sim 10^8$ s^{-1}

for alkyl ketones. However, the $S_1(^1n\pi^*) \rightarrow T_2(^3\pi\pi^*)$ ISC process happens with high efficiency due to a strong spin–orbit interaction.[37] For $C_6H_5COCH_3$, the $S_1 \rightarrow T_2$ ISC process was measured to have a rate (k_{ISC}) of $\sim 10^{11}$ s^{-1}. The T_2/T_1 crossing point is a conical intersection between the T_2 and T_1 surfaces, and the time scale for the $T_2 \rightarrow T_1$ internal conversion (IC) process via the conical intersection is expected to be on the order of a vibrational period. Therefore, the existence of the $S_1/T_2/T_1$ intersection results in the $S_1 \rightarrow T_1$ process taking place via the T_2 state. The T_2 state functions as a relay and enables the $S_1 \rightarrow T_1$ ISC to take place with a high rate. This is the reason the S_1 state lifetime for aromatic ketones is much shorter than that for aliphatic ketones, aromatic carbonyl compounds are highly phosphorescent, but only weakly fluorescent molecules, and Norrish type I and II reactions occur only from the lowest triplet state for most of aromatic ketones.

Summary and Outlook

We have shown that optically dark intermediates and intersection structures involved in radiationless transitions for aromatic carbonyl compounds can be accurately determined by high-level ab initio calculations. These dark structures are essential to understanding mechanistic photochemistry of a polyatomic molecule. Experimentally, however, it is very difficult or impossible to observe optically dark structures directly. The importance of ab initio determination of transient structures in the photodissociation dynamics has been demonstrated for the case of the aromatic carbonyl compounds. Actually, theoretical calculations are at the heart of exploring photodissociation dynamics. In addition, the detailed knowledge of mechanistic photochemistry for aromatic carbonyl compounds provides the basis for the development of our understanding of the spectroscopy, photochemistry, and photophysics of polyatomic molecules. Looking further into the future, theoretical calculations provide not only new insights into experimental findings but also some guidance to experimental study of photodissociation dynamics. Work along this line is currently underway.

BIOGRAPHICAL INFORMATION

Wei-Hai Fang was born in Anhui, China (1955). He completed his B.S. degree (1982) at Fuyang Normal University. He did his

Ph.D. work during 1990−1993 at the Beijing Normal University with Professor Ruo-Zhuang, Liu. After his postdoctoral work at Bonn University with Professor Sigid Peyerimhoff (a Humboldt Fellow), he joined the faculty of the Department of Chemistry, Beijing Normal University, in 1998 as a full professor. His main research interest is in ab initio study on mechanistic photochemistry of a polyatomic molecule.

FOOTNOTES

*Tel: 0086-10-58805382. Fax: 0086-10-58802075. E-mail: Fangwh@bnu.edu.cn.

REFERENCES

1 Schinke, R. *Photodissociation Dynamics*; Cambridge University Press: Cambridge, U.K., 1993; pp 1–15.

2 Donaldson, D. J.; Tuck, A. F; Vaida, V. Atmospheric photochemistry via vibrational overtone absorption. *Chem. Rev.* **2003**, *103*, 4717–4729.

3 Matsumi, Y.; Kawasaki, M. Photolysis of atmospheric ozone in the ultraviolet region. *Chem. Rev.* **2003**, *103*, 4767–4781.

4 Cohen, R. C.; Murphy, J. G. Photochemistry of NO_2 in earth's stratosphere: Constraints from observations. *Chem. Rev.* **2003**, *103*, 4985–4998.

5 Crespo-Hernandez, C. E.; Cohen, B.; Hare, P. M.; Kohler, B. Ultrafast excited-state dynamics in nucleic acids. *Chem. Rev.* **2004**, *104*, 1977–2019.

6 Lee, I-R.; Lee, W.; Zewail, A. H. Primary steps of the photoactive yellow protein: isolated chromophore dynamics and protein directed function. *Proc. Natl. Acad. Sci. U.S.A.* **2006**, *103*, 258–262.

7 Sinicropi, A.; Andruniow, T.; Ferre, N.; Basosi, R.; Olivucci, M. Properties of the emitting state of the green fluorescent protein resolved at the CASPT2//CASSCF/CHARMM level. *J. Am. Chem. Soc.* **2005**, *127*, 11534–11535.

8 Mitschke, U.; BaEuerle, P. The electroluminescence of organic materials. *J. Mater. Chem.* **2000**, *10*, 1471–1507.

9 Adachi, S-I.; Park, S-Y.; Tame, J. R. H.; Shiro, Y.; Shibayama, N. Direct observation of photolysis-induced tertiary structural changes in hemoglobin. *Proc. Natl. Acad. Sci. U.S.A.* **2003**, *100*, 7039–7044.

10 Heintz, O.; Robert, D.; Weber, J. V. Comparison of the degradation of benzamide and acetic acid on different TiO_2 photocatalysts. *J. Photochem. Photobiol. A: Chem.* **2000**, *135*, 77–80.

11 Srinivasan, R.; Feenstra, J. S.; Park, S. T.; Xu, S. J.; Zewail, A. H. Dark structures in molecular radiationless transitions determined by ultrafast diffraction. *Science* **2005**, *307*, 558–563, and references therein.

12 Feenstra, J. S; Park, S. T.; Zewail, A. H. Excited state molecular structures and reactions directly determined by ultrafast electron diffraction. *J. Chem. Phys.* **2005**, *123*, 221104.

13 Park, S. T.; Feenstra, J. S; Zewail, A. H. Ultrafast electron diffraction: Excited state structures and chemistries of aromatic carbonyls. *J. Chem. Phys.* **2006**, *124*, 174707 and references therein.

14 Yin, H. M.; Kable, S. H.; Zhang, X.; Bowman, J. M. Signatures of H_2CO photodissociation from two electronic states. *Science* **2006**, *311*, 1443–1446.

15 Houston, P. L.; Kable, S. H. Photodissociation of acetaldehyde as a second example of the roaming mechanism. *Proc. Natl. Acad. Sci. U.S.A.* **2006**, *103*, 16079–16082.

16 Horspool, W.; Armesto, D. *Organic Photochemistry: A Comprehensive Treatment*; Ellis Horwood Limited: Chichester, England, 1992; pp 160–200.

17 Person, M. D.; Kash, P. W.; Butler, L. J. A new class of Norrish type I process: α-bond cleavage upon $^1[n,\pi^*(C=O)]$ excitation in the acid halides. *J. Phys. Chem.* **1992**, *96*, 2021–2023.

18 Winter, P. R.; Rowland, B.; Hess, W. P.; Radziszewski, J. S.; Nimlos, M. R.; Ellison, G. B. UV photodissociation of matrix-isolated propionyl chloride. *J. Phys. Chem. A* **1998**, *102*, 3238–3248.

19 Fang, W.-H.; Liu, R.-Z. Ab initio studies of dissociation pathways on the ground- and excited-state potential energy surfaces for HFCO. *J. Chem. Phys.* **2001**, *115*, 5411–5417.

20 Fang, W.-H.; Liu, R.-Z.; Zheng, X.-M.; Phillips, D. L. Photodissociation of acetic acid in the gas phase: An ab initio study. *J. Org. Chem.* **2002**, *67*, 8407–8415.

21 Ding, W.-J.; Fang, W.-H.; Liu, R.-Z. Selectivity of the α and β bond fissions for bromoacetyl chloride upon n→π* excitation: A combined CASSCF and MR-SDCI study. *J. Chem. Phys.* **2002**, *117*, 8745–8753.

22 Wagner, P. J. Type II photoelimination and photocyclization of ketones. *Acc. Chem. Res.* **1971**, *4*, 168–177.

23 Wagner, P. J.; McGrath, J. M. Competitive types I and II photocleavage of α,α-dimethylvalerophenone. *J. Am. Chem. Soc.* **1972**, *94*, 3849–3851.

24 Lewis, F. D.; Hilliard, T. A. Photochemistry of methyl-substituted butyrophenones. *J. Am. Chem. Soc.* **1972**, *94*, 3852–3857.

25 Wagner, J. 1,5-Biradical and five-membered ring generated by δ-hydrogen abstraction in photoexcited ketones. *Acc. Chem. Res.* **1989**, *22*, 83–91.

26 Ohmori, N.; Suzuki, T.; Ito, M. Why does intersystem crossing occur in isolated molecules of benzaldehyde, acetophenone, and benzophenone. *J. Phys. Chem.* **1988**, *92*, 1086–1093.

27 Zepp, R. G.; Gumz, M. M.; Miller, W. L.; Gao, H. Photoreaction of valerophenone in aqueous solution. *J. Phys. Chem. A* **1998**, *102*, 5716–5723.

28 Takahashi, K.; Watanabe, T.; Kohtani, S.; Nakagaki, R. Photochemistry of large ring 2-phenylcycloalkanone in the presence of molecular oxygen. *J. Photochem. Photobiol. A: Chem.* **2007**, *186*, 290–297.

29 Fang, W.-H.; Phillips, D. L. The crucial role of the $S_1/T_2/T_1$ intersection in the relaxation dynamics of aromatic carbonyl compounds upon n→π* excitation. *Chem. Phys. Chem.* **2002**, *3*, 889–892.

30 Fang, W.-H.; Phillips, D. L. Photochemistry of butyrophenone and its α-substituted derivative: A theoretical examination of new photochemical route to cyclopropane group formation. *J. Theor. Comput. Chem.* **2003**, *2*, 23–31.

31 Wang, Y.-W.; He, H.-Y.; Fang, W.-H. An accurate prediction of adiabatic excitation energies to the low-lying electronic states for acetophenone and the related carbonyl compounds. *J. Mol. Struct. (THEOCHEM)* **2003**, *634*, 281–287, and references therein.

32 He, H.-Y.; Fang, W.-H.; Phillips, D. L. Photochemistry of butyrophenone: Combined complete-active-space self-consistent field and density functional theory study of Norrish type I and II reactions. *J. Phys. Chem. A* **2004**, *108*, 5386–5392.

33 East, A. L. L; Liu, H.; Lim, E. C.; Jensen, P.; Dechene, I.; Zgierski, M. Z.; Siebrand, W.; Bunker, P. R. Toluene internal-rotation: Measurement and simulation of the high-resolution S_1—S_0 fluorescence excitation spectrum at 0.5 K. *J. Chem. Phys.* **2000**, *112*, 167–175.

34 Silva, C. R.; Reilly, J. P. Theoretical calculations on excited electronic states of benzaldehyde and observation of the $S_2 \leftarrow S_0$ jet-cooled spectrum. *J. Phys. Chem.* **1996**, *100*, 17111–17123, and references therein.

35 Molina, V.; Merchan, M. Theoretical analysis of the electronic spectra of benzaldehyde. *J. Phys. Chem. A.* **2001**, *105*, 3745–3751, and references therein.

36 Page, C. S.; Olivucci, M. Ground and excited state CASPT2 geometry optimizations of small organic molecules. *J. Comput. Chem.* **2003**, *24*, 298–309.

37 Turro, N. J. *Modern molecular photochemistry*; The Benjamin/Cummings Publishing Company, Inc: Menlo Park, CA, 1978; pp 165–190.